

**Report No. FHWA-KS-99-2**  
**Final Report**

# **ACCELERATED TESTING FOR STUDYING PAVEMENT DESIGN AND PERFORMANCE**

**Hani Melhem**  
**Kansas State University**  
**Manhattan, Kansas**



**May 1999**

<b>1. Report No.</b> FHWA-KS-99-2		<b>2. Government Accession No.</b>		<b>3. Recipient Catalog No.</b>	
<b>4 Title and Subtitle</b> ACCELERATED TESTING FOR STUDYING PAVEMENT DESIGN AND PERFORMANCE				<b>5 Report Date</b> May 1999	
				<b>6 Performing Organization Code</b>	
<b>7. Author(s)</b> Hani G. Melhem				<b>8 Performing Organization Report No. 282</b> FHWA-KS-99-2	
<b>9 Performing Organization Name and Address</b> Kansas State University Department of Civil Engineering Manhattan, Kansas 66506				<b>10 Work Unit No. (TRAIS)</b>	
				<b>11 Contract or Grant No.</b> C1020; C1059	
<b>12 Sponsoring Agency Name and Address</b> Federal Highway Administration 3300 SW Topeka Blvd., Suite 1 Topeka, Kansas 66611				<b>13 Type of Report and Period Covered</b> Final Report 1997 to 1999	
				<b>14 Sponsoring Agency Code</b>	
<b>15 Supplementary Notes</b> Prepared in cooperation with the Federal Highway Administration.					
<b>16 Abstract</b>  This report describes the experimental investigation related to four experiments selected by the Midwest States Accelerated Testing Pooled Funds Program for FY 97 and FY 98. These experiments are: <ol style="list-style-type: none"> <li>1. ATL-97-1: Comparison of SM-2C and BM-2C Asphalt Overlays on Existing Portland Cement Concrete Pavement (PCCP).</li> <li>2. ATL-97-2: Comparison of PCCP jointed slabs with Fiber Reinforced Polymer (FRP) and epoxy-coated steel dowels.</li> <li>3. ATL-98-1: Comparison of an 8 in.-thick Asphalt Concrete (AC) with 5 in AC on 5 in. Reclaimed Asphalt Pavement (RAP).</li> <li>4. ATL-98-2: Performance of a rehabilitation of the pavement sections of the experiment in (3).</li> </ol> <p>The report contains a discussion of the various experimental activities, a detailed description of the experiments and a summary of the results obtained. The report includes an overview of the facility followed by the accomplishments pertaining to the individual experiments (one chapter for each experiment).</p>					
<b>17 Key Words</b> Asphalt, Portland Cement Concrete Pavement (PCCP), Fiber-Reinforced Polymer (FRP), Asphalt Concrete (AC), Reclaimed Asphalt Pavement (RAP), Falling Weight Deflectometer (FWD)			<b>18 Distribution Statement</b> No restrictions. This document is available to the public through the National Technical Information Service, Springfield, Virginia 22161		
<b>19 Security Classification (of this report)</b> Unclassified		<b>20 Security Classification (of this page)</b> Unclassified		<b>21 No. of pages</b> 110	<b>22 Price</b>

**Final Report on**

**Accelerated Testing for Studying Pavement  
Design and Performance  
(FY 97-98)**

prepared by

Hani Melhem

Department of Civil Engineering  
Kansas State University  
Manhattan, KS 66506

prepared for

Midwest Accelerated Testing Pooled Fund Study

Project Monitor:  
Richard McReynolds

May 1999

## **NOTICE**

**The authors and the State of Kansas do not endorse products or manufacturers. Trade and manufacturers names appear herein solely because they are considered essential to the object of this report.**

**This information is available in alternative accessible formats. To obtain an alternative format, contact the Kansas Department of Transportation, Office of Public Information, 7th Floor, Docking State Office Building, Topeka, Kansas, 66612-1568 or phone (785)296-3585 (Voice) (TDD).**

## **DISCLAIMER**

**The contents of this report reflect the views of the authors who are responsible for the facts and accuracy of the data presented herein. The contents do not necessarily reflect the views or the policies of the State of Kansas. This report does not constitute a standard, specification or regulation.**

## **Abstract**

This report describes the experimental investigation related to four experiments selected by the Midwest States Accelerated Testing Pooled Funds Program for FY 97 and FY 98. These experiments are:

1. ATL-97-1: Comparison of SM-2C and BM-2C Asphalt Overlays on Existing Portland Cement Concrete Pavement (PCCP).
2. ATL-97-2: Comparison of PCCP jointed slabs with Fiber Reinforced Polymer (FRP) and epoxy-coated steel dowels.
3. ATL-98-1: Comparison of a 203 mm (8 in.)-thick Asphalt Concrete (AC) with 127 mm (5 in.) AC on 127 mm (5 in.) Reclaimed Asphalt Pavement (RAP).
4. ATL-98-2: Performance of a rehabilitation of the pavement sections of the experiment in (3).

The report contains a discussion of the various experimental activities, a detailed description of the experiments, and a summary of the results obtained. The report includes an overview of the facility followed by the accomplishments pertaining to the individual experiments (one chapter for each experiment).

## **Acknowledgments**

The cooperation of the following KSU professors is here acknowledged: Dr. Stuart Swartz, Dr. Mustaque Hossain, and Dr. Hugh Walker. The dedication of Paul Lewis, Research Technologist at the Accelerated Testing Lab (ATL), is much appreciated.

The research experiments described in this report were selected, designed, and monitored by the members of the Midwest States Accelerated Testing Pooled Funds Technical Committee. The committee includes Mr. Andrew Gisi from the Kansas Department of Transportation (KDOT), Chair, Mr. George Woolstrum from the Nebraska Department of Roads (NDOR), Mr. Tom Keith from the Missouri Department of Transportation (MoDOT), and Mr. Champak Noratam from the Iowa Department of Transportation (Iowa DOT). Their help, input, and support are acknowledged.

Special thanks are due to KDOT personnel especially the Falling Weight Deflectometer (FWD) crew, and to the many KSU Civil Engineering graduate students who helped with this work, especially Mr. Xinhua Yu and Mr. Jianzhou Chen. Several undergraduate student have helped at the ATL throughout the duration of these experiments, particularly Mr. Jason Hoy (graduating senior) who worked several years at the facility, Mr. Jeffrey Davies who helped with data collection and classification, and Mr. Frederick Sheffield who worked on graphics generation and manuscript editing.

## Table of Contents

Abstract .....	-ii-
Acknowledgments.....	-iii-
List of Figures .....	-vi-
List of Tables .....	-ix-
1.0 OVERVIEW OF THE TEST FACILITY .....	1
1.1 Laboratory Space and Test Pits .....	1
1.2 Test Frame .....	2
1.3 Wheel Load Assembly .....	2
1.4 Pulse Load System.....	5
1.5 Heating and Cooling Systems .....	5
1.5.1 Glycol System with Boiler/Chiller .....	5
1.5.2 Infrared Radiant Heaters.....	7
1.6 Water Table and Soil Moisture Control .....	10
2.0 COMPARISON OF SM-2C AND BM-2C ASPHALT OVERLAYS .....	11
2.1 Pavement Structure .....	11
2.2 Soil and Subbase.....	11
2.3 Section Construction.....	12
2.4 Testing Conditions.....	13
2.4.1 Temperature Application.....	13
2.4.2 Load Application .....	13
2.5 Experiment Monitoring.....	13
2.6 Pavement Performance .....	15
2.7 Results and Conclusions .....	15
3.0 COMPARISON OF PCCP JOINTED SLABS WITH FRP AND STEEL DOWELS.....	20
3.1 Pavement Structure .....	20
3.2 Soil and Subbase.....	20
3.3 Section Construction.....	21
3.4 Testing Conditions.....	22
3.4.1 Load Application .....	22
3.4.2 Temperature Application.....	25
3.5 Experiment Monitoring.....	28
3.5.1 Instrumentation .....	28
3.5.1.1 Thermocouples.....	28
3.5.1.2 Displacement gages.....	29
3.5.2 Monitoring Plan .....	29
3.6 Pavement Performance .....	34
3.6.1 Vertical Displacement .....	34
3.6.2 Load Transfer Efficiency .....	35
3.6.3 Joint Movement.....	35
3.6.4 Slab Curling .....	39
3.7 Results and Conclusions .....	42
3.7.1 Test Results.....	42
3.7.2 Post Mortem Investigation.....	42

3.7.3 Conclusion.....	43
4.0 COMPARISON OF A 203 mm (8 in) AC WITH 127 mm (5 in) AC ON 127 mm (5 in) RAP Pavement Section.....	47
4.1 Pavement Structure.....	47
4.2 Soil and Subgrade.....	47
4.3 Testing Conditions .....	48
4.3.1 Load Application .....	48
4.3.2 Temperature Application .....	48
4.4 Experiment Monitoring.....	49
4.4.1 Instrumentation.....	49
4.4.1.1 Strain Gauges .....	49
4.4.1.2 Thermocouples .....	51
4.4.1.3 Soil Pressure Cells .....	51
4.4.1.4 Moisture Sensors .....	52
4.4.2 Monitoring Plan.....	52
4.5 Pavement Performance .....	53
4.5.1 Horizontal Tensile Strains .....	54
4.5.2 Pavement Temperature .....	54
4.5.3 Vertical Soil Pressure .....	56
4.5.4 Asphalt Concrete Density .....	56
4.5.5 Pavement Surface Rutting.....	58
4.5.5.1 Transverse Profiles .....	58
4.5.5.2 Longitudinal Profiles .....	60
4.5.5.3 Cores .....	60
4.6 Conclusions.....	60
5.0 PERFORMANCE OF A TYPICAL PAVEMENT REHABILITATION .....	63
5.1 Pavement Structure.....	63
5.2 Specimen Preparation.....	63
5.3 Testing Conditions .....	64
5.4 Experiment Monitoring.....	65
5.5 Pavement Performance.....	65
5.5.1 Horizontal Tensile Strains .....	65
5.5.2 Pavement Temperature .....	68
5.5.3 Vertical Soil Pressure .....	68
5.5.4 Asphalt Concrete Density .....	68
5.5.5 Pavement Surface Rutting.....	72
5.5.5.1 Transverse Profiles .....	72
5.5.5.2 Longitudinal Profiles .....	72
5.6 Conclusions.....	72
APPENDIX A: MARSHALL MIX DESIGN DATA .....	74
APPENDIX B: TYPICAL RESULTS FROM ATL-98-1 EXPERIMENT .....	79
APPENDIX C: SURFACE PROFILES FOR ATL-98-2 EXPERIMENT .....	93
References.....	99

## List of Figures

	<u>Page</u>
Figure 1.1 Test Frame and Wheel Load Assembly	3
Figure 1.2 Wheel Assembly and Tandem Axles	4
Figure 1.3 Wheel Assembly Completing One Repetition	4
Figure 1.4 Reaction Frame and Pulse Load System Configuration	6
Figure 1.5 Close-up Actuators and Hydraulic Hose Assembly	7
Figure 1.6 Test Pit Heat Exchanger Detail	8
Figure 1.7 Glycol System's Pipe Supply to Testing Pit	9
Figure 1.8 Surface Glycol Cooling/Heating Thermal Panels	9
Figure 2.1 Plan of the AC Slabs	12
Figure 2.2 Load Application of Wheel Carriage Cycles (November 1997)	14
Figure 2.3 Tandem Axle Load Applied to Overlays Under Radiant Heater Directed to the Wheel Paths at 122°F	14
Figure 2.4 Performance Monitoring Plan	15
Figure 2.5 SM-2C Slabs' Rutting Effects Per Number of Cycles	17
Figure 2.6 BM-2C Slabs' Rutting Effects Per Number of Cycles	18
Figure 2.7 Changes of AC Modulus in SM-2C and BM-2C Slabs	19
Figure 2.8 Changes of PCC Modulus in SM-2C and BM-2C Slabs	19
Figure 3.1 Cyclic Load Simulation Produced by Two Actuators	23
Figure 3.2 Mechanical Device for the Pulse Load System	24
Figure 3.3 Mechanical Device with Load Cells and Servo-Valves	25
Figure 3.4 Testing Pit with Loading Beams and Surface Panels	27
Figure 3.5 Test Specimen with Loading Beams, Surface Panels and Heaters	28
Figure 3.6 Locations of Thermocouples	30
Figure 3.7 Locations of Dial Indicators	31
Figure 3.8 Monitoring / Testing Plan	32

## List of Figures (Continued)

	<u>Page</u>	
Figure 3.9	Average Thermocouple Layer Temperatures	33
Figure 3.10	Load vs. Deflection after 200,000 Cycles (Gage 1)	34
Figure 3.11	Comparing Stiffness of Steel and FRP Dowels	36
Figure 3.12	Variation of Load Transfer Efficiency with Respect to Number of Load Cycles	37
Figure 3.13	North Profiles (Steel)	40
Figure 3.14	South Profiles (FRP)	41
Figure 3.15	Pictures of Push-Out Bar Testing (a-d)	44,45
Figure 4.1	Location of Sensors in Nebraska Test (ATL-98-1)	50
Figure 4.2	Variation of Peak Strains with Number of Load Repetitions	55
Figure 4.3	Variation of Peak Pressure with Number of Load Repetitions	57
Figure 4.4	Variation of Asphalt Concrete Density with Number of Load Repetitions	59
Figure 4.5	Location of Drilled Cores	61
Figure 5.1	Specimen After Milling of Entire Pavement	64
Figure 5.2	Variation of Peak Strains with Number of Load Repetitions	67
Figure 5.3	Thermocouple Readings for ATL-98-2 Experiment	69
Figure 5.4	Variation of Peak Pressure with Number of Load Repetitions	70
Figure 5.5	Variation of Asphalt Concrete Density with Number of Load Repetitions	71
Figure B.1	Strain Gage Data at 1000 Load Reps for Strain Gage #1	80
Figure B.2	Full Trace of Two Complete Cycles	81
Figure B.3	Comparison of Strains Between 7,500 and 25,000 Repetitions (Load Repetition at 18 kips)	82
Figure B.4	Thermocouple Readings for ATL-98-1 Experiment	83
Figure B.5	Pressure Sensor Data at 1000 Load Repetitions for Pressure Sensor #1	84

### List of Figures (Continued)

	<u>Page</u>	
Figure B.6	Average Trace of Two Complete Cycles	85
Figure B.7	Comparison of Pressure Between 7,500 and 25,000 Repetitions (Load Repetitions at 18 kips)	86
Figure B.8	Comparison of Pressure Between 1,000 and 25,000 Reps (1,000 Load Reps at 8 kips / 25,000 Reps at 18 kips)	87
Figure B.9	Transverse Profiles (East)	88
Figure B.10	Transverse Profiles (Middle)	89
Figure B.11	Transverse Profiles (West)	90
Figure B.12	Longitudinal Profiles (North Slab)	91
Figure B.13	Longitudinal Profiles (South Slab)	92
Figure C.1	Transverse Profiles (East)	94
Figure C.2	Transverse Profiles (Middle)	95
Figure C.3	Transverse Profiles (West)	96
Figure C.4	Longitudinal Profiles (North Slab)	97
Figure C.5	Longitudinal Profiles (South Slab)	98

## List of Tables

	<u>Page</u>	
Table 2.1	Progression of Rutting on the Primary Sections	16
Table 2.2	Progression of Rutting	16
Table 2.3	Maximum Rutting as a Function of Mixture Properties	16
Table 3.1	Measured Joint Movement Due to Change in Temperature	38
Table 3.2	Measured Joint Movement Due to Change in Temperature	38
Table 3.3	Measured Joint Movement Due to Change in Temperature	39
Table 3.4	Summary of Plan, Schedule, and Tests for Field Program	46
Table 4.1	Monitoring Plan for ATL-98-1 Experiment	53
Table 5.1	Monitoring / Testing Plan for ATL-98-2 Experiment	66

## 1.0 OVERVIEW OF THE TEST FACILITY

A detailed description of the facility can be found in reference (1). This chapter presents an overview of the main features of the Kansas Accelerated Testing Lab (K-ATL) including new improvements to the equipment and additional capabilities implemented at the lab since the original report was prepared.

The K-ATL is part of a broader facility named the “Kansas State University Testing Laboratory for Civil Infrastructure.” The facility also includes the Kansas Falling Weight Deflectometer (FWD) state calibration room, and a shake-table for structural dynamic testing and earthquake engineering research. The FWD room is adjacent to the main testing lab and the shake-table is installed in an empty test pit, similar to those filled with compacted soil and used for pavement testing.

### 1.1 Laboratory Space and Test Pits

The laboratory area consists of about 537 m<sup>2</sup> (5775 sq. ft) of test space which includes the main test area of about 418 m<sup>2</sup> (4500 sq. ft) with the test pits at the center, about 93 m<sup>2</sup> (1000 sq. ft) for the FWD calibration room, and about 26 m<sup>2</sup> (275 sq. ft) for the electrical and mechanical rooms where the pavement cooling and heating equipment is installed.

Two 1.8 m (6 ft) deep test pits are located in the center of the lab. The main pit is 9.8 m×6.1 m×1.8 m (32'×20'×6') and has been partitioned into a 6.1 m×6.1 m×1.8 m (20'×20'×6') pit for pavement testing, and a 3.7 m×6.1 m×1.8 m (12'×20'×6') pit presently used for earthquake research.

Next to this pit is an insulated environmental pit which is 6.1 m×3.7 m×1.8 m (20'×12'×6') and which has metal (stainless steel) U-tubes buried in the soil underneath the specimen and in which a glycol solution is circulated to freeze or heat both the subgrade and the slab. Adjacent to the environmental pit is a 1.2 m (4 ft) wide access pit. It is used to allow easy access to instrumentation and heating/cooling U-tubes. It currently includes the main headers used to distribute and collect the glycol solution to and from the U-tubes. The headers have ball-valves on the supply and return sides of each U-tube.

The lab floor is 457 mm (18 in.) thick throughout the ATL area and is structurally integral with the pit walls. Floor beams are buried in the concrete floor on both sides of the pit to guide the testing frame and provide attachment (tie-down) against uplift when the load is applied to the specimens. The floor design includes provisions for confining the edges of concrete slab specimens that tend to contract when cooled in the environmental pit. This simulates the thermal tensile stresses created in a section of a continuous concrete highway where the joints would restrain the contraction in the direction parallel to the highway centerline. For these reasons 19

mm (3/4") threaded rods are used to attach the test slabs to the top of the 457 mm (18 in.)-thick vertical pit walls. The rods, embedded in the concrete slabs, pass through 25 mm (1 in.)-diameter sleeves staggered at 76 mm (3 in.) intervals.

## **1.2 Test Frame**

The test frame is shown in Figure 1.1. The two main girders and four columns are made of W30×99 rolled beams. The frame span is 12.8 m (42 ft) center-to-center. This allows the carriage to get off the specimen before it hits the end of the track where a system of air springs redirect the carriage in the opposite direction.

The elevation at which the girders are connected to the columns was raised by 102 mm (4 in.) prior to testing an AC overlay that was placed over a previously tested PCCP section. The frame is designed such that the beam/column rigid connection can be altered at 76 mm (3 in.) vertical increments.

## **1.3 Wheel Load Assembly**

The test frame and loading devices were designed and fabricated by Cardwell International, Ltd., of Newton, Kansas. The wheel assembly consists of a tandem axle assembly (TAM) with air suspension system (air-bags). The wheel assembly (carriage) is an actual bogie from a standard truck (see Figure 1.2). A manually controlled air-compressor provides pressure in the air-suspension system and therefore applies load to the wheel axles. The wheel load versus air pressure relation was verified for each set of wheels using a portable weigh-scale of the local Highway Patrol authority. The air-bag pressure was increased linearly at 69 kPa (10 psi) increments and the load was recorded until it reached 178 kN (40,000 lbs), including the self weight of the bogie and reaction frame.

The arrangement allows the system to load one or both axles as desired. One or more pairs of tires may be replaced by a super-single if a test requires so. Normally the system would be loading in both direction as the wheel assembly moves back and forth. However, one-way traffic simulation can be achieved through a hydraulic system that can lift the wheel axles either manually or automatically. The automatic mode will cause the eight wheels to be lifted off the ground when the carriage reaches the end of the track until it goes back to its initial position and starts a new load cycle. The manual mode is used when the whole test frame needs to be moved off the specimen or across the laboratory space. The frame is moved by pulling it using an overhead crane. Accurate positioning is achieved manually with a pry-bar.

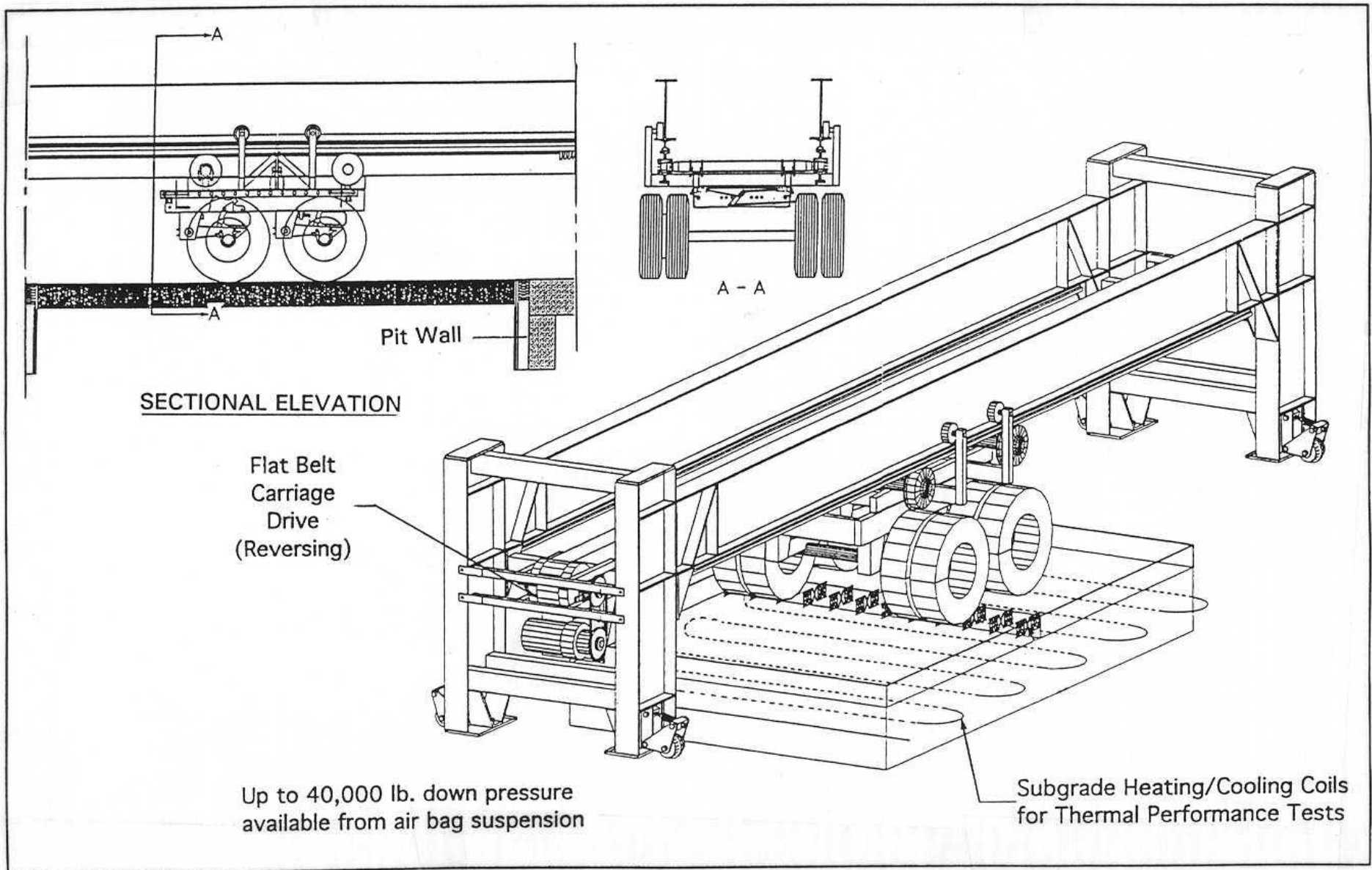


Figure 1.1 Test Frame and Wheel Load Assembly  
 (Design Provided by Cardwell International, Ltd.)



Figure 1.2 Wheel Assembly and Tandem Axles



Figure 1.3 Wheel Assembly Completing One Repetition  
(Photo taken by KSU Photographic Services)

The TAM is moved back and forth along the track using a flat conveyor belt driven by a 20 HP variable speed electric motor which reverses direction every time the carriage reached one end or the other of reaction frame (Figure 1.3). The fastest safe operating speed achieved is 300 cycles per hour, or 600 load applications per hour for the two-way passage operation. At this rate, the average speed of the wheel's axles is 5.6 km/h (3.5 mph) over the total travel distance of 9.1 m (30 ft), whereas, the speed over at least 5.5 m (18 ft) at the middle portion of the 12.8 m (42 ft) track is about 11.3 km/h (7 mph).

## **1.4 Pulse Load System**

When fatigue tests of jointed Portland Cement Concrete Pavements (PCCP) are performed, it is normally more appropriate to apply cyclic loads (thumping) across the joint using a closed-loop system with hydraulic actuators (from MTS Systems Corp.). Generally it takes several million load cycles to fail PCCP joints, as opposed to few hundred thousand to fatigue AC pavement. This has been successfully used when comparing the behavior of different shear transfer devices at a joint. Using this setup a speed of 9000 applications per hour has been achieved which is 15 times faster than the rolling axles, and many more cycles can be applied in a significantly shorter duration of time.

The same reaction frame carrying the wheel load assembly is used to support the pulse load system. The wheel carriage (bogie) is moved to one end of the frame (East end) to make room for the pulse load system at the midspan of the frame. The pulse load system consists of two actuators (cylinders) activated by a hydraulic power supply (MTS pump) and positioned across the PCCP joint (Figures 1.4 and 1.5). Each actuator applies the load on one side of the joint in an alternating fashion, such that when one cylinder is down, the other one is up. This results in a rocking action on the two half-sections of the pavement simulating the passage of a truck over the joint, even though it does not exactly replicate the rolling wheel effects.

## **1.5 Heating and Cooling Systems**

### **1.5.1 Glycol System with Boiler/Chiller**

This temperature application system uses a boiler for heating and a chiller system for cooling or freezing. They both use the same 55% ethylene glycol-based fluid that circulates in the thermal coils to heat/cool the pavement slab and/or subgrade. A set of control valves on the supply and return lines direct the solution to either the boiler or the chiller depending upon the test requirements. Temperature ranges between -23°C and +66°C (-10°F and +150°F). The depth of the pipes in the



Figure 1.4 Reaction Frame and Pulse Load System Configuration

subgrade determines how much of the soil underneath the pavement is thermally controlled. To add more flexibility to the testing facility, the elevation of the heat exchanger (piping network) varies by having six lines of holes at 203 mm (8 in.) intervals (vertically) so that when soil is removed from the pit, the pipes can be installed at a different depth. In the present initial position, 17 U-tubes are installed at the third row of holes from the top, i.e. at 914 mm (36 in.) below the lab floor level and evenly spaced horizontally at 203 mm (8 in.) intervals (Figures 1.6 and 1.7).

The capability of heating and cooling from the top through the thermal panels was added to duplicate the usual natural conditions and allow the flexibility to control the temperature gradient through the pavement surface and the subgrade. This is accomplished by circulating the glycol fluid through thermal panels (stainless steel plate coils) connected with flexible pipes so that pavement can be cooled/heated from the top down (Figure 1.8). This allows specification of the temperature of both the pavement surface and the subgrade, and hence the ability to control the temperature gradient through the pavement. A strip on the surface of the specimen can be exposed to allow for the wheel load to travel on the heated/cooled pavement after it has been heated or cooled. Each of the lower and upper systems can be operated independently. Through manipulating a set of valves, it is possible to have the top and bottom of the pavement both cooled, both heated, top heated/bottom cooled, or vice versa. Thermocouples are installed on the tubes and below and above the base and the pavement. Surface heating is also achieved by using radiant heat lamps (infrared heater). This best simulates exposures of AC pavement to direct sunlight and is used rutting tests.



Figure 1.5 Close-up Actuators and Hydraulic Hose Assembly

### 1.5.2 Infrared Radiant Heaters

This system is designed only for surface heating and uses infrared radiant heaters. It best simulates heating of a roadway surface by direct radiation from the sun. It consists of four lines mounted on supporting brackets parallel to direction of the rolling of the carriage, two for each set of wheels of the axle assembly, and one line on each side of a wheel path. A separate sensor and control unit is installed on each individual line to monitor/cycle its operation and maintain the desired surface temperature of the pavement. The lines radiate heat the full 6.1 m (20-ft) length of the wheel path, but only heat the width of the pavement at the wheel paths. Temperatures as high as 121 °C (250 °F) can be achieved, but values up to 50 °C (122°F) are more realistic for highway pavement applications.

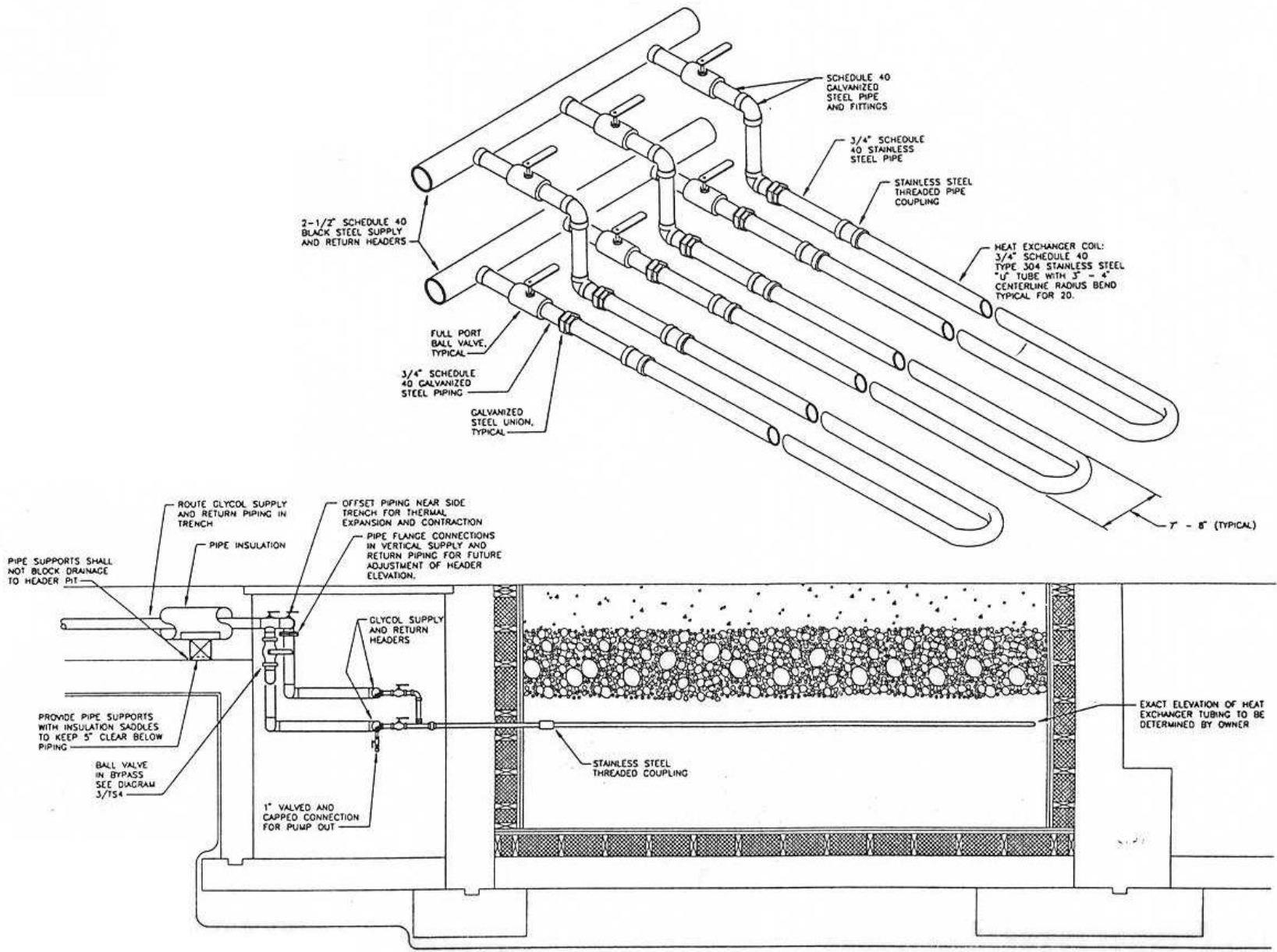


Figure 1.6 Test Pit Heat Exchanger Detail  
 (Drawing provided by Orazem & Scalora Engg)



Figure 1.7 Glycol System's Pipe Supply to Testing Pit



Figure 1.8 Surface Glycol Cooling/Heating Thermal Panels

## 1.6 Water Table and Soil Moisture Control

A sprinkler/drainage system is installed in both the middle pit and the environmental pit. The inside walls of the concrete pit were coated with a waterproof sealant, and the inside walls of the environmental pit are covered with a watertight rubber membrane to prevent water from getting into the thermal insulation. The water sprinkler consists of three soaker hoses buried right under the surface of the aggregate base, transverse to the direction of wheel rolling, and under the concrete pavement.

The location of the hoses is at 0.6 m (2 ft), 3.1 m (10 ft) i.e. at the middle, and 5.5 m (18 ft) spacing from one end or the other of the pit. The middle soaker hose was used alone during the concrete pavement test (it lays well under the PCCP joint) to achieve the most serious soil erosion and pumping action under the joint.

Three water collectors were placed horizontally at the bottom of each of the pits consisting of 102 mm (4 in.) perforated black plastic pipes (corrugated) leading into a metal riser tube of 254 mm (10 in.) diameter installed vertically at one corner of each pit. A layer of 279 mm (11 in.) of UD-1 or pea gravel was laid at the bottom of both pits to facilitate water drainage. Filter fabric was then placed on top of the gravel. With the riser tubes, the water level can be observed from the surface and excess water can be removed by dropping a sump pump to the bottom when necessary. TDR (Time Domain Reflectometry) is used to measure the soil moisture at the beginning of testing and at regular intervals as water is added to the subgrade.

## 2.0 COMPARISON OF SM-2C AND BM-2C ASPHALT OVERLAYS

This chapter describes the first experiment performed under the fiscal year 97 contract (ATL-97-1) which is the third experiment conducted at the facility (ATL-Exp#3). This was the first experiment of the Midwest Accelerated Pooled Fund study.

The purpose of this experiment is to compare KDOT Superpave SM-2C mix design with KDOT Marshall BM-2C mix design when used as asphalt concrete overlays over existing PCCP. The two different types of mixes were placed side-by-side over the three previously tested PCCP sections (ATL-Exp #2) in the large pit (6.1 m x 9.8 m x 1.8 m) of the ATL.

### 2.1 Pavement Structure

The asphalt overlays were about 100 mm (4 in.) thick and were placed as three adjacent lanes of about 1.9 m (76 in.)-wide each on top of the existing 230 mm (9 in.) concrete sections. Each of the three 6.1 m-long (20 ft) strips was divided into two sections placed parallel to the direction of the rolling wheels. The two sections consist of mixes prepared with optimum and optimum +0.5% binder content as shown in Figure 2.1.

### 2.2 Soil and Subbase

The *granular subbase* is crushed limestone placed in loose lift thickness of 152 mm (6 in.) and compacted to 95% of the maximum dry density (MDD) of 2323 kg/m<sup>3</sup> (145 pcf). The optimum moisture content of this aggregate base (KDOT AB-3) material was approximately 10%. The subbase was stabilized at optimum +2% moisture content.

*Subgrade soil* of 1220 mm (48 in.)-thick was placed and compacted on top of the 279 mm (11 in.) of pea gravel that was put at the bottom of the pit for drainage. It was a typical silty soil (AASHTO A-4) from a borrow pit placed in approximately 152 mm (6 in.) lifts and compacted to 90% of the laboratory MDD. Its liquid limit, plasticity index, sieve analysis, MDD, and optimum moisture content (OMC) were calculated in the Materials lab at KSU. The density obtained was monitored with a nuclear gage. The top 457 mm (18 in.) of the subgrade was compacted to 95% of MDD. The in-place moisture content of the subgrade was measured with Time Domain Reflectometry (TDR) waveguides as 15.5% during construction and decreased to about 10.5% three months later.



BM-2C Optimum binder content ↑ Rolling	SM-2C Optimum binder content ↑ Direction of wheel	BM-2C Optimum binder content ↑ Assembly
① BM-2C Optimum +0.5 % 20,000 Rep.	③ SM-2C Optimum +0.5 % 80,000 Rep. 20,000 Rep.	② BM-2C Optimum +0.5 % 80,000 Rep

Figure 2.1 Plan of the AC Slabs

### 2.3 Section Construction

The BM-2C was placed first on the south and north lanes then saw-cut to width to make room in-between for the SM-2C that was placed in the central lane the next day. The south lane was placed unintentionally by mistake of the contractor but it was left in place as an additional replicate. The PCCP under the south lane had a failed joint with X-FLEX as shear transfer device, the one under the central lane has an unbroken joint with FiberCon, and that under the north lane had an unbroken joint with standard epoxy-coated steel dowels.

### 2.4 Testing Conditions

### **2.4.1 Temperature Application**

During the application of the axle loads, the pavement was constantly heated at 50°C (122°F) from the surface with the infrared radiant heaters. The four thermal sensors that monitor the operation of the heaters controlled surface temperature. Therefore, temperature on the pavement surface was always around 50°C (122°F) and never went below or above this value by more than a couple of degrees. Also, temperatures along the wheel path were periodically measured using an infrared hand-held thermometer (Raytek ST6). No provisions were made to read or monitor the temperature below the surface and in the subbase. Heaters were turned on before testing and load application would start when the surface temperature reached the desired temperature. Starting at room temperature, it took between 15 and 30 minutes to reach the 50°C (122°F).

### **2.4.2 Load Application**

The strips were tested in pairs such that two adjacent lanes were each loaded with one half tandem axle. The rolling wheel tandem axle was used in this experiment. The design tandem axle load was 151 KN (34,000 lbs). The testing frame was moved laterally every so many cycles to simulate wander of the traffic on the pavement. The lateral movement is applied at seven discrete intervals with a number of cycles in each interval that represent the random (normal) distribution of the traffic, as shown in the histogram of Figure 2.2. The carriage and consequently the center of each pair of wheels were therefore moved according to this distribution within a 3 ft-wide range ( $\pm 1.5$  ft from central position).

This has proven to be very efficient when testing asphalt pavement to avoid excessive rutting that would be obtained if the wheels were always traveling on the same fixed path. However, the testing machine was not designed to allow for lateral wander of the load axles and this operation had to be done manually which is quite labor intensive and did slow down the testing operation considerably. The wheel carriage and radiant heater are shown in Figure 2.3 in operation during testing.

## **2.5 Experiment Monitoring**

The performance monitoring plan is shown in Figure 2.4. It included measuring transverse and longitudinal profiles at one foot intervals using a Face Dipstick, density measurement with a nuclear gauge, and recording deflections with the KDOT Falling Weight Deflectometer (FWD) device. The frequency and locations of these measurements were performed as indicated in the table of Figure 2.4.

For each 10,000 repetitions:

Displ. (ft)	-1.5	-1	-0.5	0	0.5	1	1.5	Sum =
No. Rep.	712	1,316	1,899	2,146	1,899	1,316	712	10,000

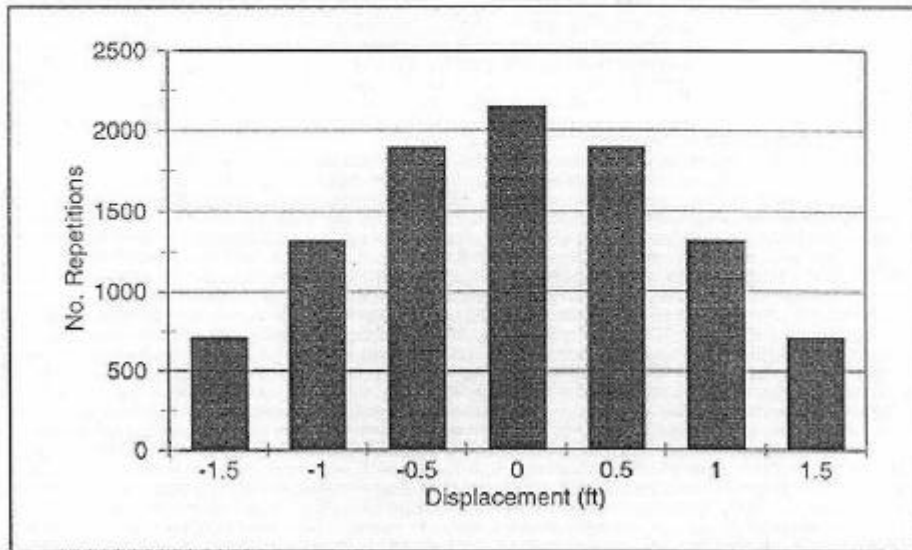


Figure 2.2 Load Application of Wheel Carriage Cycles (November 1997).



Figure 2.3 Tandem Axle Load Applied to Overlays Under Radiant Heater Directed to the Wheel Paths at 122°F.

No. of Repetitions	Monitored Distress or Response/Monitoring Agency				
	Rutting*/ Transverse Profile/ KSU (Dipstick)	Nuclear ** Density/ KSU	Cracking/ KSU	Longitudinal Profile***/ KSU (Dipstick)	Surface Deflection by FWD****/ KDOT
0	✓	✓	-	✓	✓
10,000	✓	✓	✓	✓	✓
50,000	✓	✓	✓	✓	✓
100,000	✓	✓	✓	✓	✓

Figure 2.4 Performance Monitoring Plan

- \* at the middle of each test section (5 ft from the east or west end)
- \*\* at 1 ft intervals (longitudinally), 3 ft from the edge on each test section (initial location of the center of left tire (looking west) of the tandem assembly)
- \*\*\* at 3 ft from the north/south edge on each test section
- \*\*\*\* at 3 ft from the north/south edge on each test section, with the load plate 3 ft from the west/east test section end and then 5 ft from the east/west edge of the test section. Target loads 7, 9 and 15 kips.

## 2.6 Pavement Performance

The progression of rutting in both the SM-2C and the North BM-2C slabs is shown in Tables 2.1 and 2.2 as well as in Figures 2.5 and 2.6. The maximum rutting as a function of mixture properties is given in Table 2.3. Changes in the modulus of the AC and that of the underlying PCC layer are shown in Figures 2.7 and 2.8.

## 2.7 Results and Conclusions

The central and north lanes were tested first for up to 80,000 cycles. At that stage rutting in the north lane was about 30.5 mm (1.2 in., see Figure 2.9). Therefore the tandem axle was moved over the central and south lanes that were tested for an additional 20,000 cycles. The north lane therefore had 80,000 cycles, while the central lane had a total of 100,000 cycles and the south lane had 20,000 cycles.

From visual inspection and by examining the rutting profiles, it can be concluded that the sections with optimum binder content performed slightly better than those with optimum content +0.5 percent. Moreover, it appears that the SM-2C mix tested has a better rut resistance than the BM-2C.

FWD data and density values were given to KDOT and were further analyzed at KSU in a different research project. Results will appear elsewhere as a separate publication.

Table 2.1 Progression of Rutting on the Primary Sections

Section Type	Section Location	Approximate Maximum Rut Depth (inches) @ Repts.			
		10,000	20,000	50,000	80,000
BM-2C	NW	0.10	0.30	0.65	0.80
SM-2C	CE	0.15	0.40	0.60	1.00
BM-2C+0.5%	NE	0.25	0.50	0.75	1.25
SM-2C+0.5%	CW	0.30	0.40	0.55	0.90

Table 2.2 Progression of Rutting on all Sections

Section Type	Section Location	Approximate Maximum Rut Depth (inches) @ Repts		
		0	20,000	80,000
BM-2C	NW	0	0.30	0.75
BM-2C	SW	0	0.10	---
BM-2C+0.5%	NE	0	0.50	1.25
BM-2C+0.5%	SE	0	0.30	---
SM-2C	CE	0	0.40	1.1
SM-2C+0.5%	CW	0	0.30	0.9

Table 2.3 Maximum Rutting as a Function of Mixture Properties

Section Type	Section Location	Max. Rut Depth (inches)	PCC Modulus, psi (millions)	Air Voids (%)	VMA (%)	VFA (%)	% Coarse River Sand
BM-2C	NW	0.80	—	1.93	10.5	81.2	6
SM-2C	CE	1.00	—	2.37	11.3	79	13
BM-2C+0.5%	NE	1.25	2.96	2.12	11.3	81.6	6
SM-2C+0.5%	CW	0.90	4.06	1.56	12.3	87.3	13

**Key:** NE: North East      CE: Center East      NW: North West  
 SE: South East      CW: Center West      SW: South West

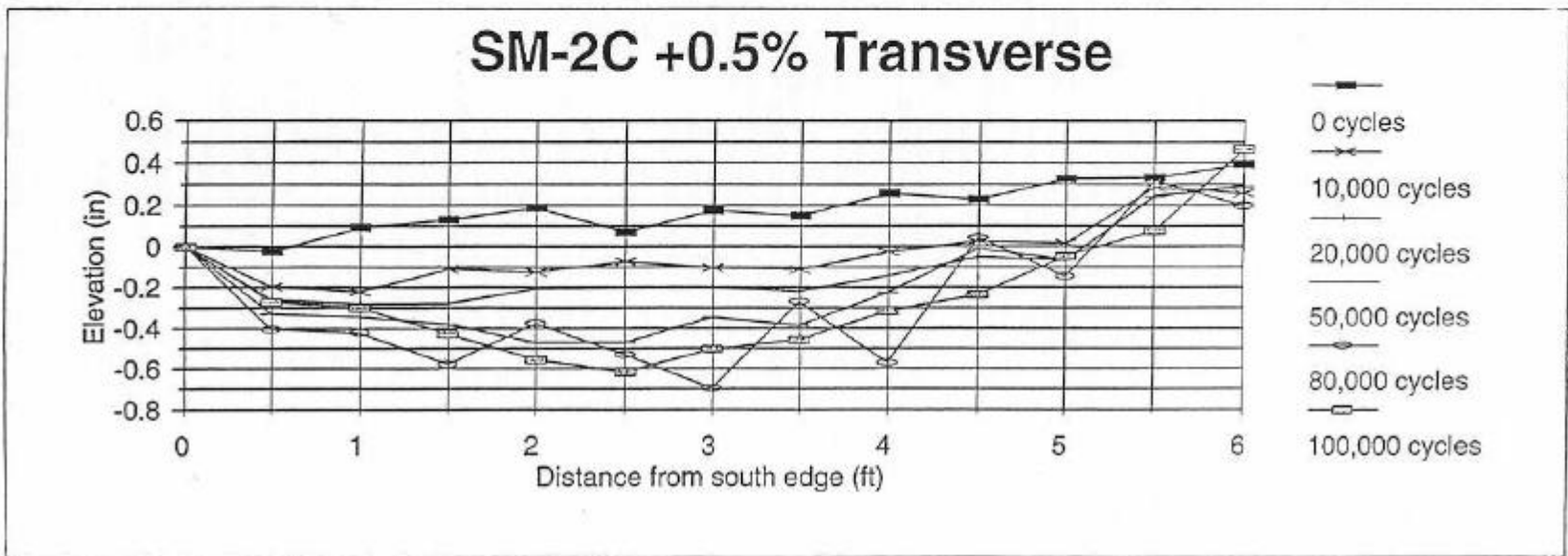
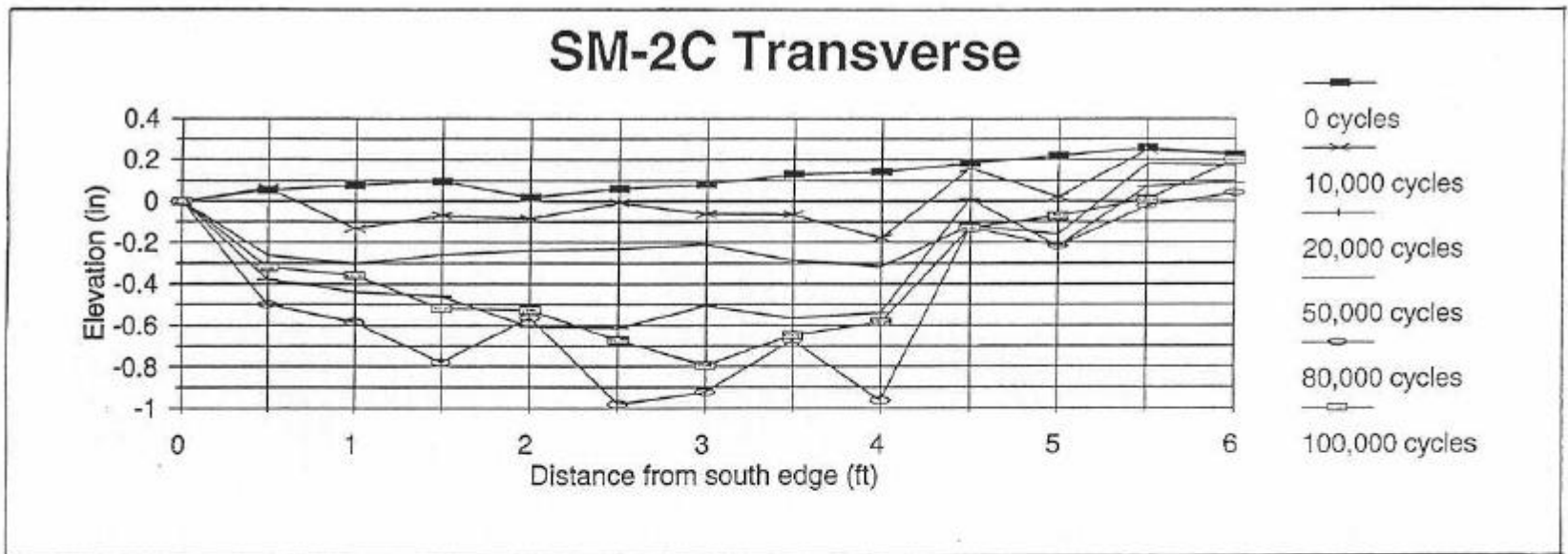


Figure 2.5 SM-2C Slabs' Rutting Effects Per Number of Cycles

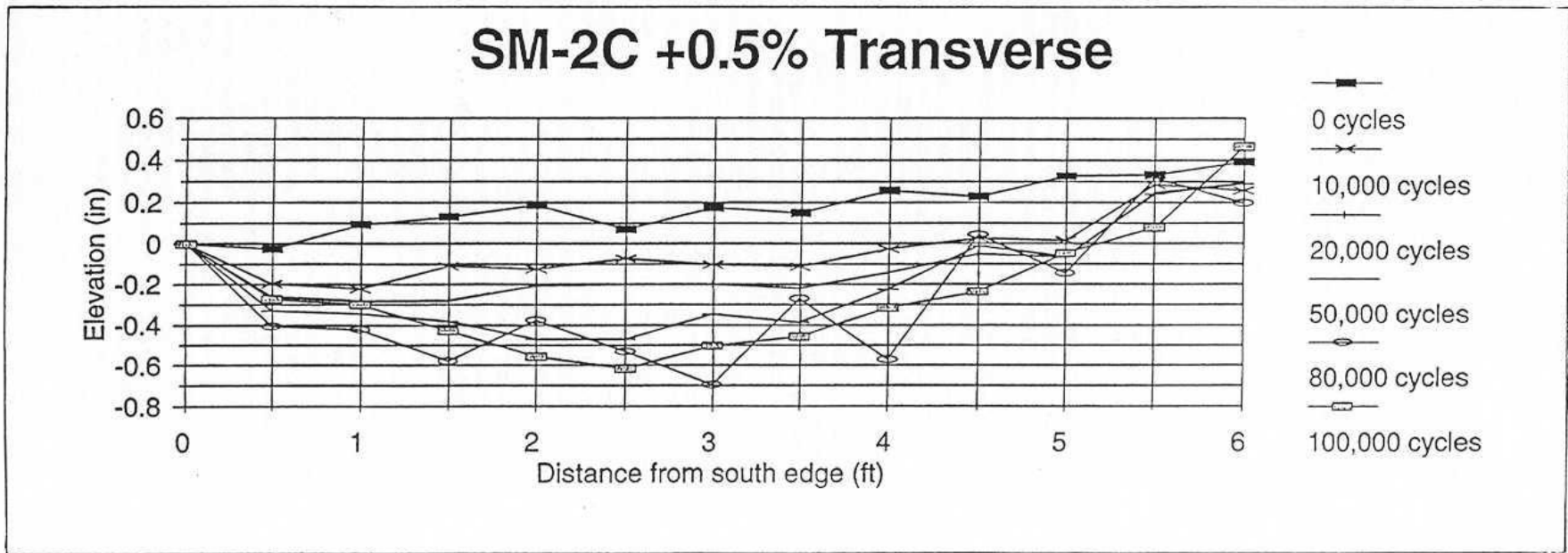
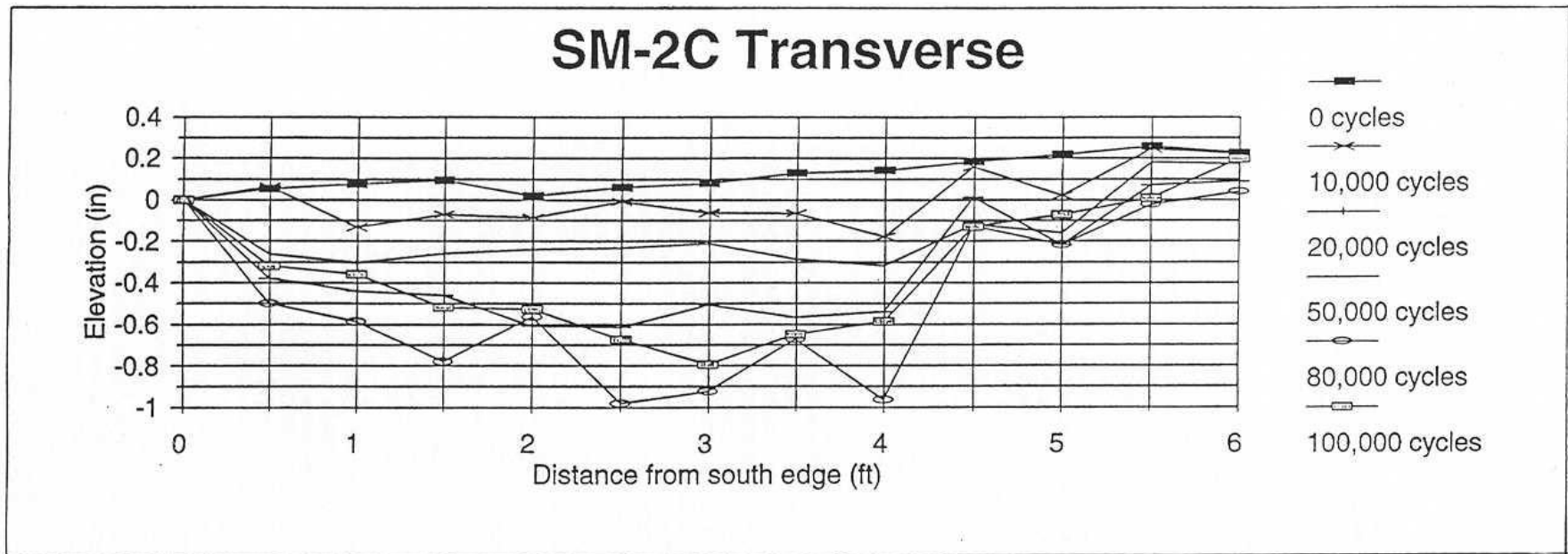


Figure 2.6 BM-2C Slabs' Rutting Effects Per Number of Cycles

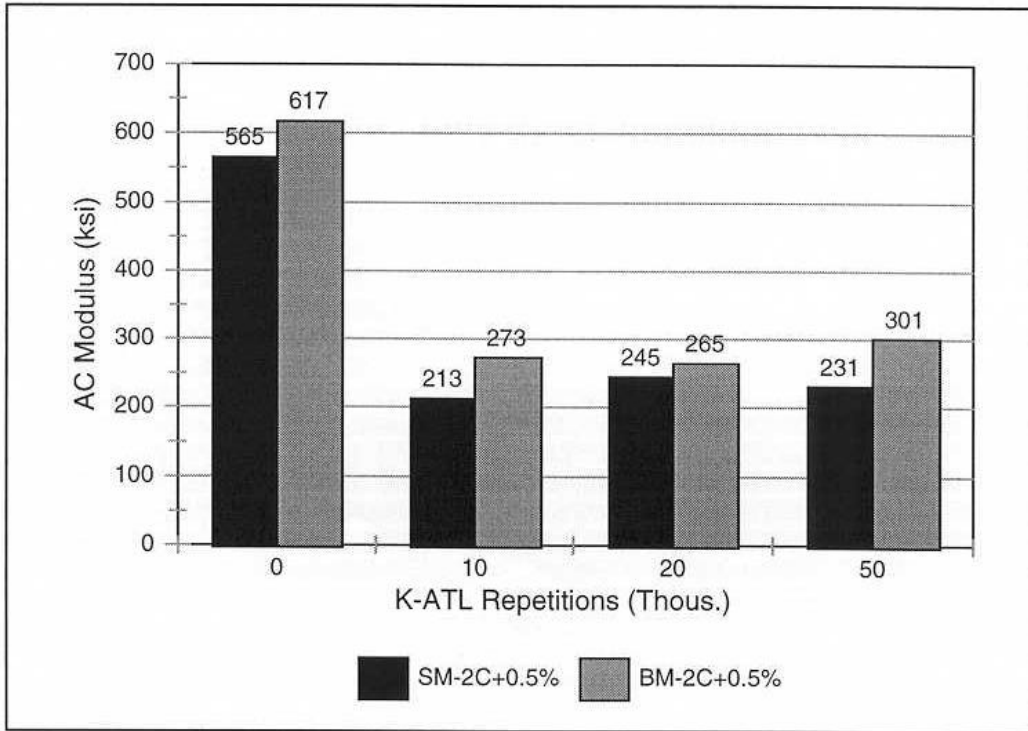


Figure 2.7 Changes of AC Modulus in SM-2C and BM-2C Slabs

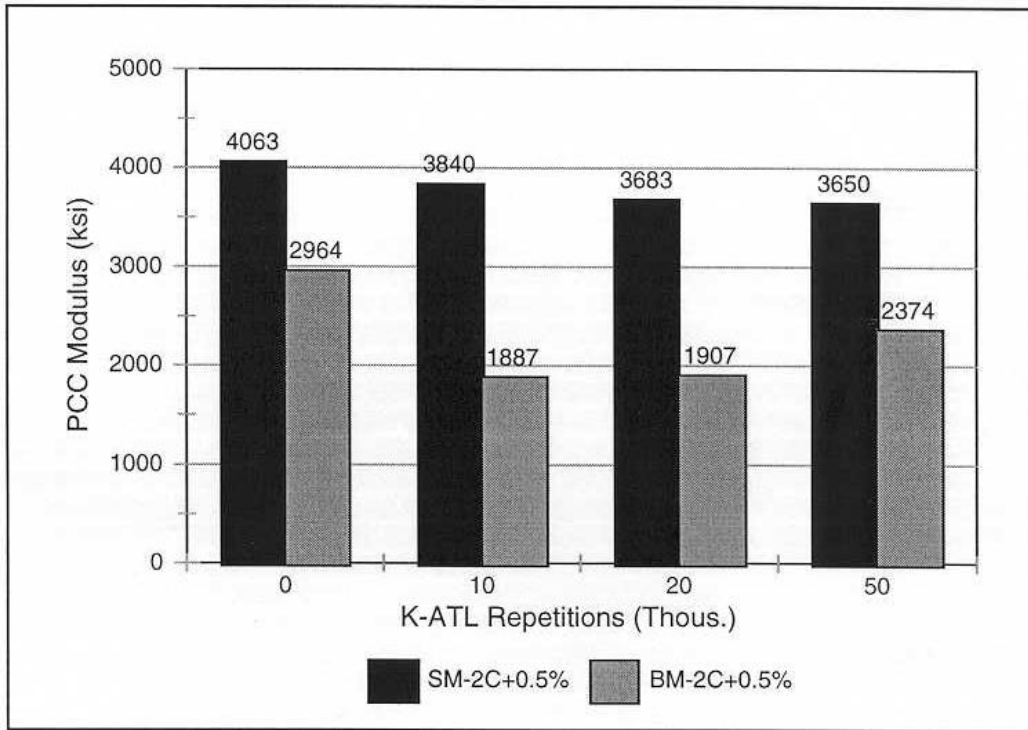


Figure 2.8 Changes of PCC Modulus in SM-2C and BM-2C Slabs

### **3.0 COMPARISON OF PCCP JOINTED SLABS WITH FRP AND STEEL DOWELS**

This chapter describes the second experiment performed under the fiscal year 97 contract (ATL-97-2), which is the fourth experiment conducted at the facility (ATL-Exp#4). This was the experiment was funded by the Midwest Accelerated Pooled Fund study.

The purpose of this experiment is to compare the performance of Fiber Reinforced Polymer dowels with standard epoxy-coated steel dowels in PCCP joints. Two jointed slabs were placed side-by-side in the north (environmental) pit of the K-ATL. This was the first experiment at the K-ATL to be conducted in the environmental pit.

#### **3.1 Pavement Structure**

The pavement structure consists of 200 mm (8 in.)-thick non-reinforced Portland Cement Concrete slabs with lateral joints at midspan. The north slab had 25 mm (1 in.)-diameter epoxy-coated steel dowels at the joint and the south slab had 38 mm (1.5 in.)-diameter fiberglass dowels. The slabs were placed on a well-compacted layer of aggregate base consisting of 100 mm (4 in.) of AB-3.

#### **3.2 Soil and Subbase**

The pit depth-profile (from bottom to top) is as follows:

The bottom (and four sides) of the pit has a 200 mm (8 in.) thick wood frame enclosing styro-foam thermal insulation. Then comes the 280 mm (11 in.) of pea gravel (covered by a filter fabric). On the top of the gravel, 355 mm (14 in.) of the same soil used in the middle pit was placed and compacted. Then 75 mm (3 in.)-thick insulation panels were placed side-by-side and covered with black tar for additional thermal insulation. On top of the panels, about one inch of sand (on average) was placed to level the surface so that the stainless-steel U-tubes of the heat exchanger could be laid.

The U-tubes are located at 915 mm (36 in.) from the top of the pit or lab floor level. About 610 mm (24 in.) of subgrade soil has been placed and compacted above the U-tubes topped by 100 mm (4 in.) of AB-3 base and the 200 mm (8 in.) slabs.

### 3.3 Section Construction

The two slabs were separated longitudinally by a gap created by 2×8 timber dividers that were removed after the concrete had cured. Timber form-work was also placed along the sidewalls of the testing pit and removed after construction to ensure that the slabs are free to expand and contract. Vertical stakes used to hold the timber were placed through holes drilled in the timber itself, and not next to it, to avoid any possible friction or holding around the slab edges. All interior sides of the form-work (towards the concrete slab) were greased including both sides of the middle longitudinal divider. All form-work was removed before loads were applied, creating a 50.8 mm (2 in.) gap between the two slabs and between the slabs and the pit sidewalls. These gaps also allow seeing the aggregate base, water level, and any cracks in the slabs.

The 25.4 mm (1 in.) diameter epoxy coated steel dowel bars came with their own basket as standard welded contraction joint assembly Type “J” from Dayton Superior. Before casting the concrete the longitudinal wires were cut off. These wires were parallel to the dowels and their role was to hold the basket together during shipping and handling. The 38.1 mm (1.5 in.) FRP dowels, 457 mm (18 in.) long, came from Glassform Inc., and were placed using two individual single stakes Type “FS” per dowel, also from Dayton Superior. Dowel spacing was 305 mm (12 in.) for both types of dowels.

To ensure that the construction of the FRP joint was comparable to that of the steel joint (in which the steel bars are welded at one end to the basket) one end of the FRP dowels was glued with fiberglass epoxy resin to the FS stake holding it at this end. As in the case of the steel basket assembly, this end attachment was staggered between consecutive bars. A thin film of grease was applied on half the length of the dowels (both the steel and FRP) from the middle of the dowel length to the free end (staggered). Also to avoid bearing stresses due to thermal expansion when slabs were heated during testing, round pieces of foam of 25.4 mm (1 in.) and 38.1 mm (1.5 in.) diameter were glued to the free ends of the steel and FRP dowel bars, respectively.

At the time of placing, the Portland cement concrete had an air entrainment of 3.6% and a slump of 105 mm (4-1/8 in.). Cylinder tests at 28-days showed the concrete had a compressive strength of 38.53 MPa (5588 psi). On the second day, concrete was saw-cut in one stage to a depth of 76.2 mm (3 in.) at the joint. The surface of the concrete was covered with plastic sheets for a period of 10 days after placement to ensure proper curing at room temperature.

The experiment benefited from the ATL floor design that includes provisions for confining the edges of a concrete slab specimen that would expand or contract under varying temperature in the environmental pit. In particular, when cooled or due to shrinkage during curing, the slabs tend to contract. In a real-life situation, such a slab will be a section of a continuous concrete highway, and the section

under consideration would be prevented from contraction in the direction parallel to the highway centerline. For this reason threaded bars were used to attach the test slab to the pit vertical walls at the two ends perpendicular to the direction of traffic. (The tops of these pit walls have sleeves designed for this purpose.) These end-anchors consisted of 19 mm ( $\frac{3}{4}$  in.) diameter threaded rods placed in one row at 152 mm (6 in.) spacing, center-to-center. They penetrate in the concrete slabs about 457 mm (18 in.). Nuts were placed at the other end of the wall and snug-tightened two days after the concrete was poured. Additional torque was applied to these nuts progressively on subsequent days as the concrete cured.

Like many instances during PCCP construction, at first the slab did not completely crack (through the full depth) at the joint due to concrete shrinkage. It was therefore necessary to make sure that the crack from the saw-cut propagates to the bottom of the slab, below the level of the dowels. This was verified by adding water in the crack after forming a small reservoir with water-tight dams in the surface crack. To achieve this, a sequence of steps was used. First, the slabs were cooled to 4.4°C (40°F). Then a small cyclic load was applied incrementally right at the joint, up to 25% of the magnitude of the load used later during testing. A few hundred cycles were applied using 2×4 pieces of wood placed on top of the joints, right along the joint line, to create tensile bending stresses at the bottom of the slabs. In addition to temperature and fatigue loads, the end-anchors were tightened a little further which caused the water in the crack to run down the joint, indicating that full depth cracks was formed in both slabs.

### **3.4 Testing Conditions**

The environmental pit was used for this experiment. The heating/cooling system was used to cause warping of the slab and joint movement. Axle loads were to be applied in combination with temperature cycling. Both slabs, the one with steel dowels and the one with FRP dowels, were tested side-by-side such that load was applied simultaneously.

In general the experiment called for the application of pulse loads on the jointed slab, across the joint line. Cyclic loads with maximum magnitude of 178 kN (40,000 lbs) were applied as sine-wave pulses alternating across the joints. Four footprints per side were applied simulating an single truck axle configuration. This resulted in the equivalent of a pair of wheels of 89 kN (20,000 lbs) crossing each of the two slabs (with steel and FRP dowels.)

#### **3.4.1 Load Application**

Load was applied to both sides of the joints in order to simulate truck passages over the joint. The two electronically controlled closed-loop hydraulic actuators described in Section 1.4 were used to apply the load. The load was applied by each actuator in a sinusoidal-shape function, with the two functions 180 degrees out-of-phase. Therefore when one actuator was at the maximum load on one side of the joints, the

other was at the minimum load (zero) on the other side. This loading procedure was used by many researchers studying PCCP joints such as Porter *et al.*,(1993). This is illustrated in Figure 3.1.

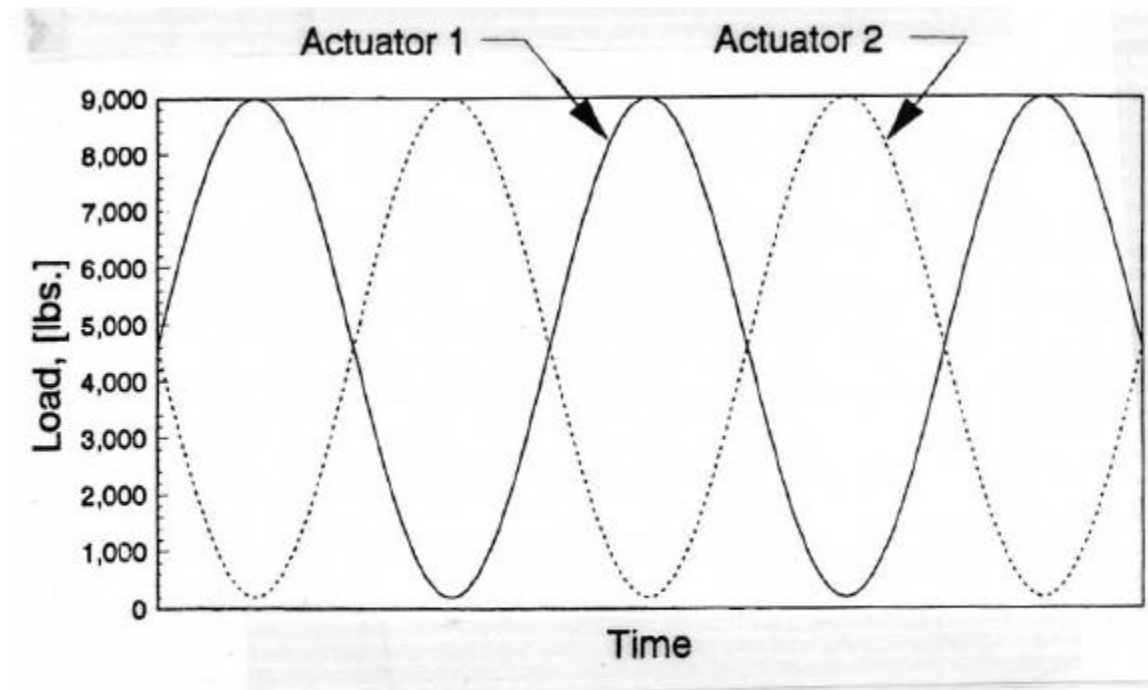


Figure 3.1 Cyclic Load Simulation Produced by two Actuators  
(Reproduced from Porter *et al.*, 1993)

The mechanical device is shown in Figure 3.2. Load cells and servo-valves (not shown in this figure) were added. These can be seen in Figure 3.3. The insulated hoses crossing over the loading beams are for circulating the glycol solution in the surface thermal panels from one coil to the other, across the loading device. Each actuator was controlled by a separate MTS servo-controller (Model 407). The controllers were programmed as master/slave units such that the main units generated the command signal and the following auxiliary unit will follow at the desired phase-shift.

The optimum testing frequency was about four cycles per second (4 Hz) which simulates 14,400 axle passages per hour. This allowed the application of 100,000 repetitions per day during working hours. Load cycles were not applied without lab personnel attendance to maintain the appropriate level of testing control and safety practices. Also at this speed, about 0.25 million cycles can be applied overnight during which a crack may occur and would be unrecorded, and the temperature conditions would not be as well monitored.

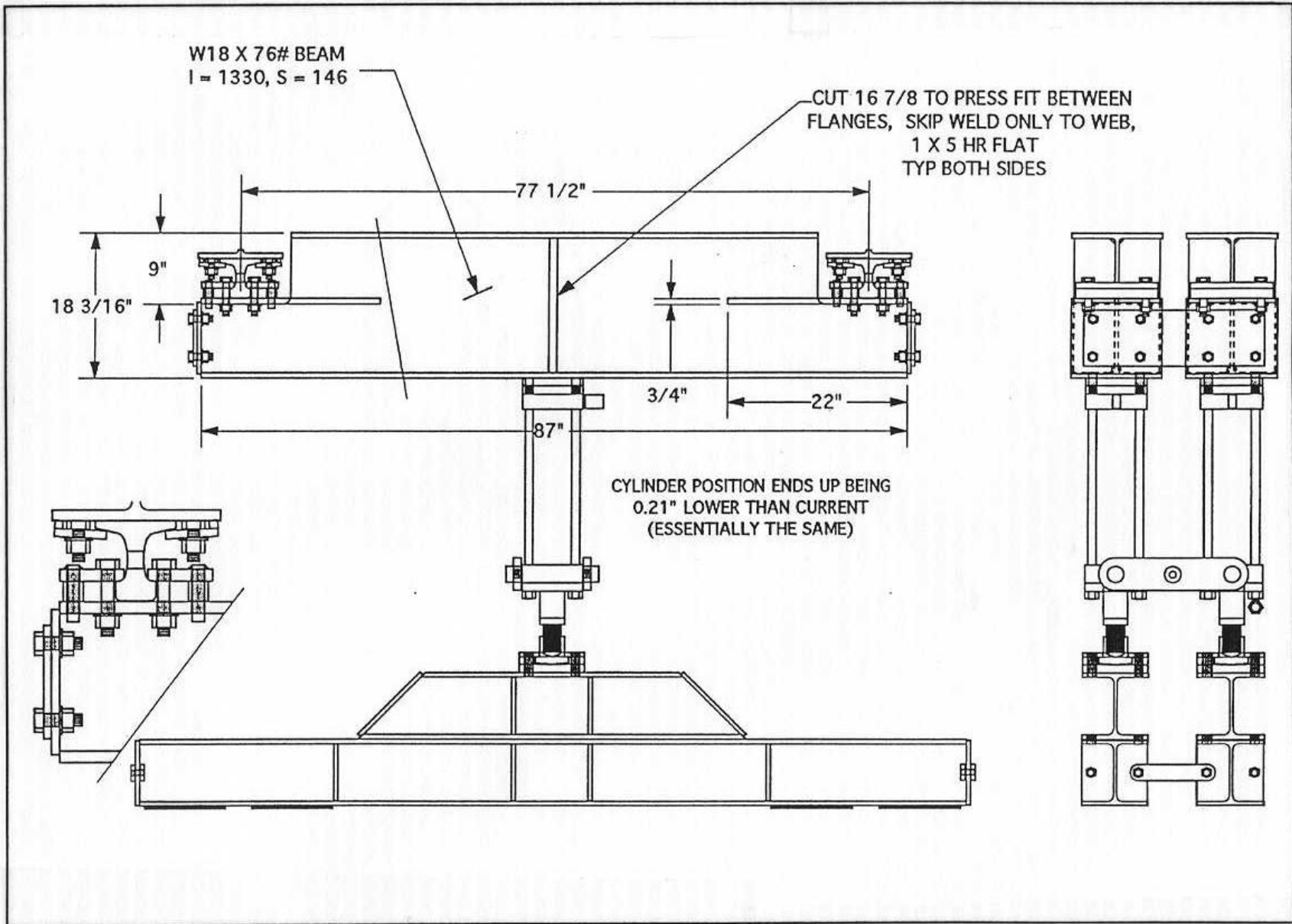


Figure 3.2 Mechanical Device for the Pulse Load System  
*(Drawing provided by Cardwell Concrete Systems)*



Figure 3.3 Mechanical Device with Load Cells and Servo-Values

### 3.4.2 Temperature Application

First, the slabs were heated and cooled from the surface and through the coils in the subgrade to ensure that both joints with the steel and FRP dowels open and close properly with temperature variation. Then it was necessary to experiment with the heating/cooling system to determine the best way/sequence of applying temperature cycling during loading.

After several days of experimenting with the system, the best procedure was determined as follows. The temperature below the pavement was kept fairly constant (lower tubes were closed) while surface temperatures were cycled. As shown in Figure 1.8 (Chapter 1), it takes 12 panels to cover the entire 3.66 m x 6.10 m (12 ft x 20 ft) pit surface since each panel is 0.610 m by 1.83 m (2 ft by 6 ft). It

was most practical to keep these panels placed on the slab during the whole test because the installation and removal of the surface coils are labor-intensive processes. This would conceal any crack or failure of the slabs. It was therefore necessary to use only eight panels and leave a 0.610 m (2 ft) wide strip uncovered on each side of the pit surface. This is illustrated in Figure 3.4 and can be seen in Figure 3.5.

The uncovered strips were also useful to measure surface longitudinal profiles (curling) using the Face Dipstick device, and to install dial gages to measure deflection and joint movement. The dipstick measurements were made along a line going through mid-width of the 0.610 m (2 ft) strips, i.e., about 0.305 m (1 ft) from the edges of the pit sidewalls or pavement slab side edges. However, if remaining uncovered, these strips would be exposed to the ambient environment thus possibly creating undesired longitudinal stresses in the PCCP slabs. It was therefore decided to use the infrared surface heater to raise the surface temperature of these strips to the same level as those covered by the panels. One line of radiant heaters was used on each side of the pit as indicated on Figure 3.4. During cooling, it was not possible to cool the slab by radiation, so it was thought that at least these strips could be temporarily covered. Fiberglass insulation material (as used for wall insulation in building construction) was used for this purpose. This was easily rolled up or down, before and after cooling, and simple to partially lift during periodical visual inspection of the slabs for cracks.

As mentioned earlier, loads were applied during regular business hours such that it took about seven hours to apply 100,000 repetitions every day. The eighth hour was used to take static deflection readings, measure profiles, perform visual inspection, and check up the equipment. By the end of the work day (around 5:00 PM) the chiller or boiler and radiant heaters were turned on or off depending upon the thermal cycling sequence. The time period during the evening and overnight helped reach the steady temperature level desired by 8:00 AM when the next set of load repetition would start.

On the first day of testing the surface temperature was kept at 37.8°C (100°F), the next day it was lowered to 21.1°C (70°F, room temperature), the third day further down to 4.44°C (40°F), and the fourth day back to 21.1°C (70°F), and so forth. Thermocouple (heat sensors) showed that temperatures remained fairly constant when the load repetitions were applied.

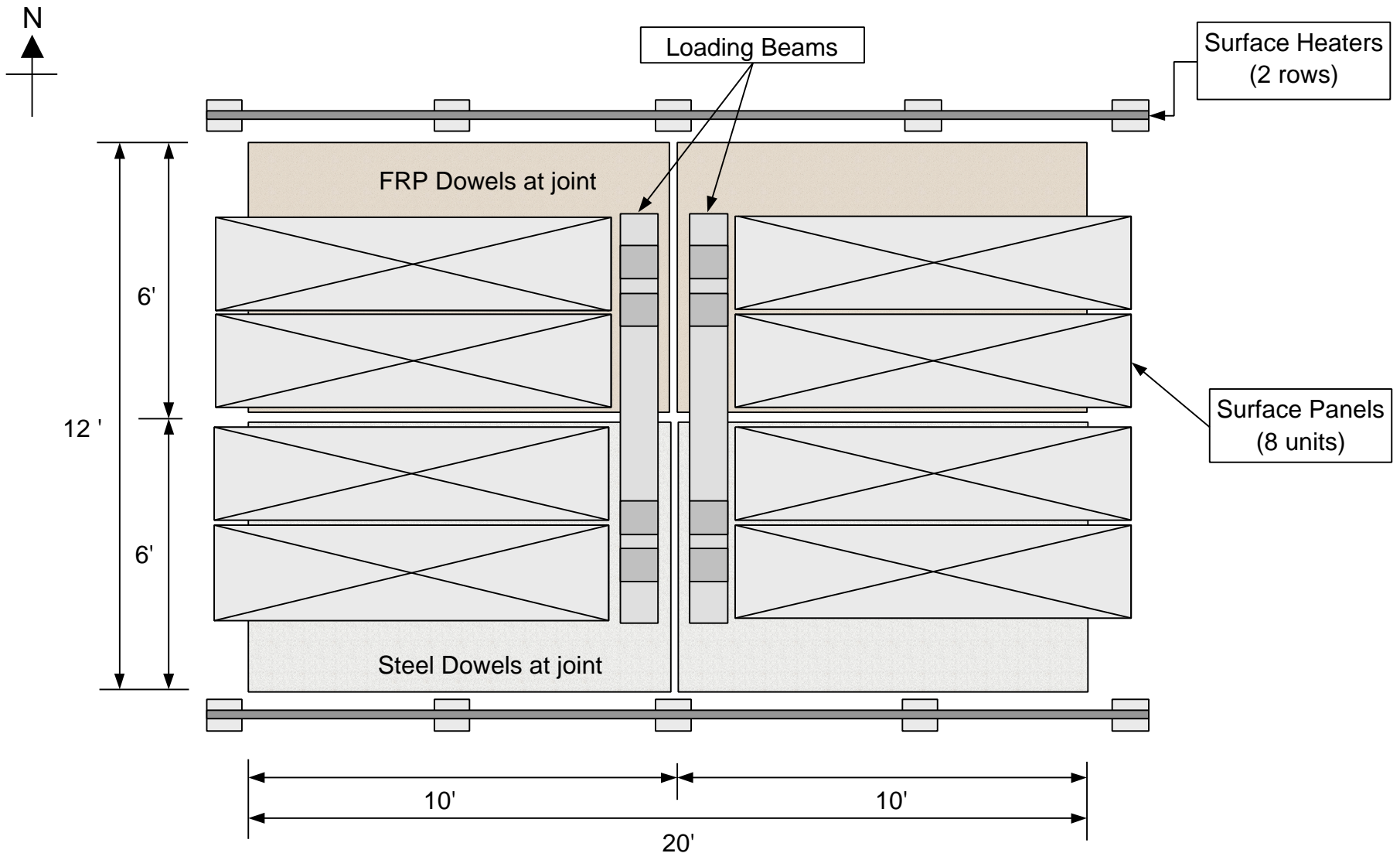


**Figure 3.4 Testing Pit with Loading Beams and Surface Panels**



Figure 3.5 Test Specimen with Loading Beams, Surface Panels, and Heaters

### **3.5 Experiment Monitoring**

This section describes the different types of instrumentation used to monitor the test and monitor the performance of the pavement.

#### **3.5.1 Instrumentation**

Monitoring the temperature in the PCCP slabs, in the subbase, and in the subgrade was the most important aspect of performance monitoring for this experiment. This was particularly crucial because it was the first experiment ever conducted in the thermal pit and the first time the chiller/boiler glycol system was used at the K-ATL.

##### *3.5.1.1 Thermocouples*

These are temperature sensors that were either imbedded in the soil and pavement or glued to the steel pipes and surface thermal panels. Temperature data are electronically recorded using a digital data acquisition system built at the K-ATL. The system uses computer Data Acquisition (DAQ) boards, specialized hardware (SCXI modules and terminal blocks), and software development packages (LabView) all from National Instruments.

A total of 31 thermocouples were used as shown in Figure 3.6. The first nine

sensors (numbered in the figure as 0 to 8) with self adhesive tabs were placed on the stainless steel U-tubes that are buried in the soil in the pit, 0.914 m (3 ft) below the floor level. They are arranged as three on the first tube by the west wall, three on the middle tube by the middle of the pit, and three on the last tube by the east wall (there are 17 U-tubes in the pit). Of these three sensors, one is at the inlet to the U, one at the middle, and the third by the outlet.

The following layer up of thermocouples (9 to 17) is at 406 mm (16 in.) from the surface. These were placed at the interface between the subgrade soil and the aggregate base. The next set up (No. 18 to 26) was placed on top of the aggregate base right below the concrete slabs. The very top set of sensors (No. 27 to 30) were glued to the bottom surface of coil panel which is in direct contact with the top surface of the slab.

The self-adhesive sensors, glued to the tubes and to the surface coils, were used to compare the temperature of the metal conduits (tubes and coils) with the temperature indicators of the glycol solution in the mechanical room at the pump where the boiler and chiller are feeding the heat exchange system. This helped regulate the flow rate, the heat exchange efficiency, and the capacity of the compressor.

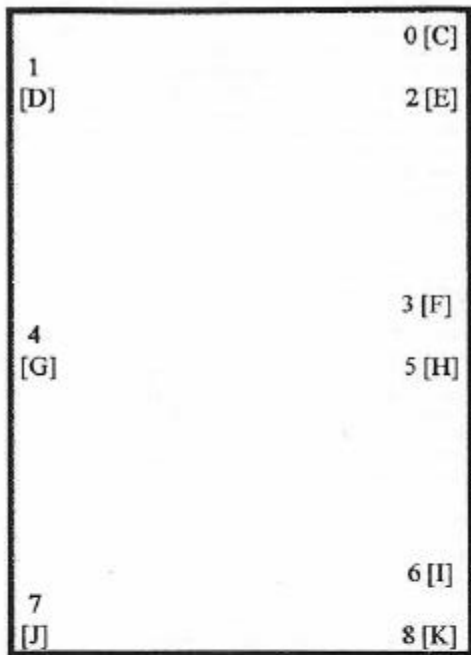
#### *3.5.1.2 Displacement gages*

These were dial indicators of accuracy of 1/25,400 mm and 1/254,000 mm (1/1,000" and 1/10,000"). They were mounted on brackets with magnetic bases. The location of these gages is shown in Figure 3.7. Gages 1 and 2 were used to measure deflection of the slab before and after the joint with steel dowels, whereas gages 3 and 4 were on the joint with FRP dowels. The tip of the gages was touching the slab surface while the base of the holding brackets was placed on the pit side walls. Therefore deflections were measured relative to the walls that are integral with the 457 mm (18 in.)-thick lab floor and virtually do not move.

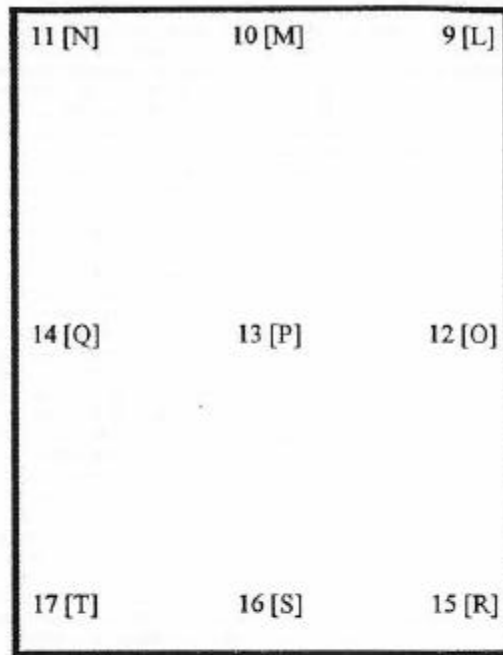
The other two gages were placed horizontally across the joints in the two slabs, respectively, and were used to measure the opening and closing of the joints when the slabs were cooled or heated.

### **3.5.2 Monitoring Plan**

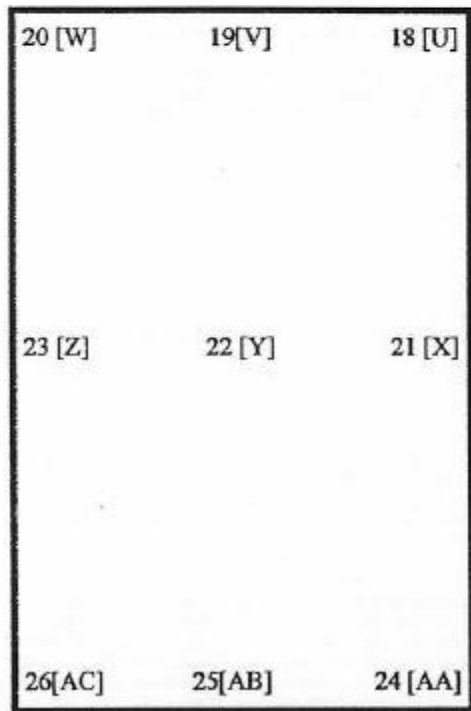
The monitoring/testing plan is shown in Figure 3.8. The numbers in the middle two columns of the table indicate the dates (in 1998) when the different activities were actually performed. For instance at zero load repetitions, vertical deflection measurements were done on June 2, dipstick profiles were measured on May 27, and FWD tests were conducted on May 26, indicated in the first row of the Table as 6/2, 5/27, and 5/26, respectively.



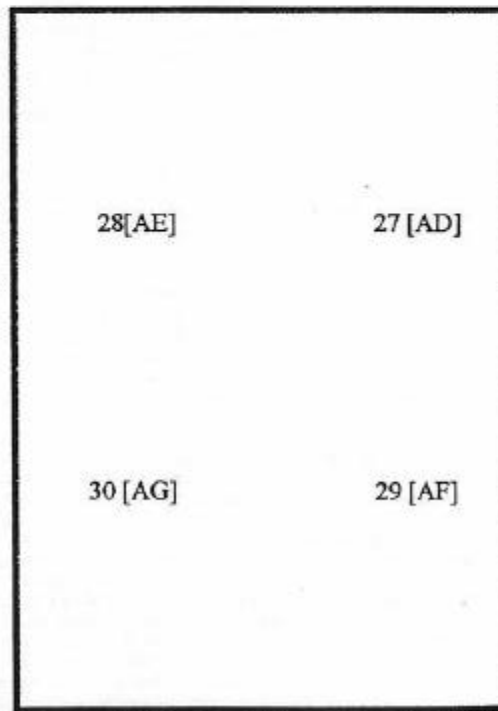
Bottom (U-tubes) level (-36")



Below AB-3 level (-16")



Below Slab level (-8")



Top of Slab - Floor level (-0")

Figure 3.6 Locations of Thermocouples

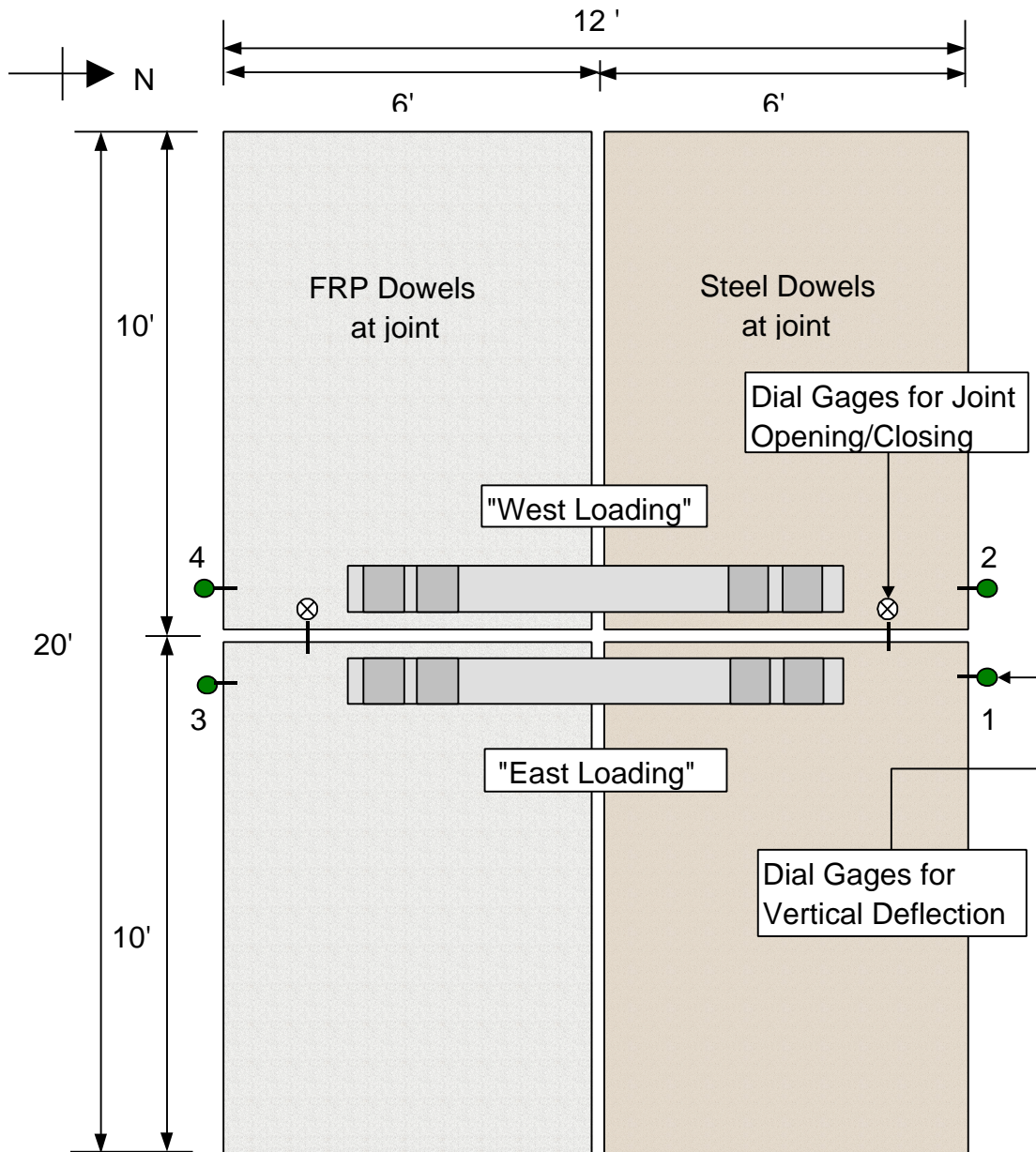


Figure 3.7 Locations of Dial Indicators

The two numbers (N/S) in the last column in the table represent the joint opening (or closing) that occurred in the North (steel doweled) and South (FRP doweled), respectively. The recorded values represent the joint movement since 5:00 p.m., when testing was completed, till the morning of the following working day when testing was about to start.

LOAD: 40,000 lb axles - load alternating across joints  
4 footprints per axle on each side of the joint

No. CYCLES: Up to 1 million load applications

TEMPERATURE: Keep lower loop temperature (soil) constant at 70°F  
Cycle surface temperature between 40°F and 100°F

N / S

Load Rep. x 10 <sup>-3</sup>	Surface <sup>1</sup> Temp. (°F)	Visual Inspection	Vertical <sup>2</sup> Deflection	Profile Dipstick	FWD tests	Joint <sup>3</sup> Opening x 10 <sup>-4</sup> (in)
0	70	OK	6/2	5/27	5/26	30 / 30
100	100	OK		6/3		60 / 60
200	70	OK	6/4	6/4		33 / 19
300	40	OK		6/5		20 / 10
400	70	OK	6/8			4 / 17
500	100	OK		6/9		24 / 40
600	70	OK	6/10			19 / 44
700	40	OK		6/11		48 / 27
800	70	OK	6/12			23 / ---
900	100	OK				34 / 51
1000	70	OK	6/16		✓	38 / 27

**Notes:**

1. Apply temperature before starting load application and keep constant throughout this step.
2. Apply static load on each side of the joint in increments of 5,000 lbs and record dial gages (0.001" accuracy) across the joints (two gages on each side).
3. Also measure joint opening (horizontal displacement) with dial gages or extensimeters as concrete is curing and as temperature is being applied.

Figure 3.8 Monitoring / Testing Plan

## Temperature Cycles

The temperatures recorded by the thermocouples are shown in Figure 3.9 for the duration of the entire experiment. The readings of the various sensors in each layer (see Figure 3.6) were averaged and plotted as a single graph line for that layer. The temperature measurements of most concern were those at the top and bottom of the slab as they are an indication of the thermal gradient across the pavement depth. As seen in the figure, the top surface temperatures are those that change the most since heat application/removal was driven from the top coils. Other thermocouple layers are shown in the graph but do not vary as much as the surface temperatures because they are placed deeper below the pavement and in the soil.

After the first slab has failed at 1.1 million cycles, the temperature was lowered to around  $-6.67^{\circ}\text{C}$  ( $20^{\circ}\text{F}$ ) for one day, then  $4.44^{\circ}\text{C}$  ( $40^{\circ}\text{F}$ ) for another day, and subsequently kept cool at  $-6.67^{\circ}\text{C}$  ( $20^{\circ}\text{F}$ ), till the end of the experiment.

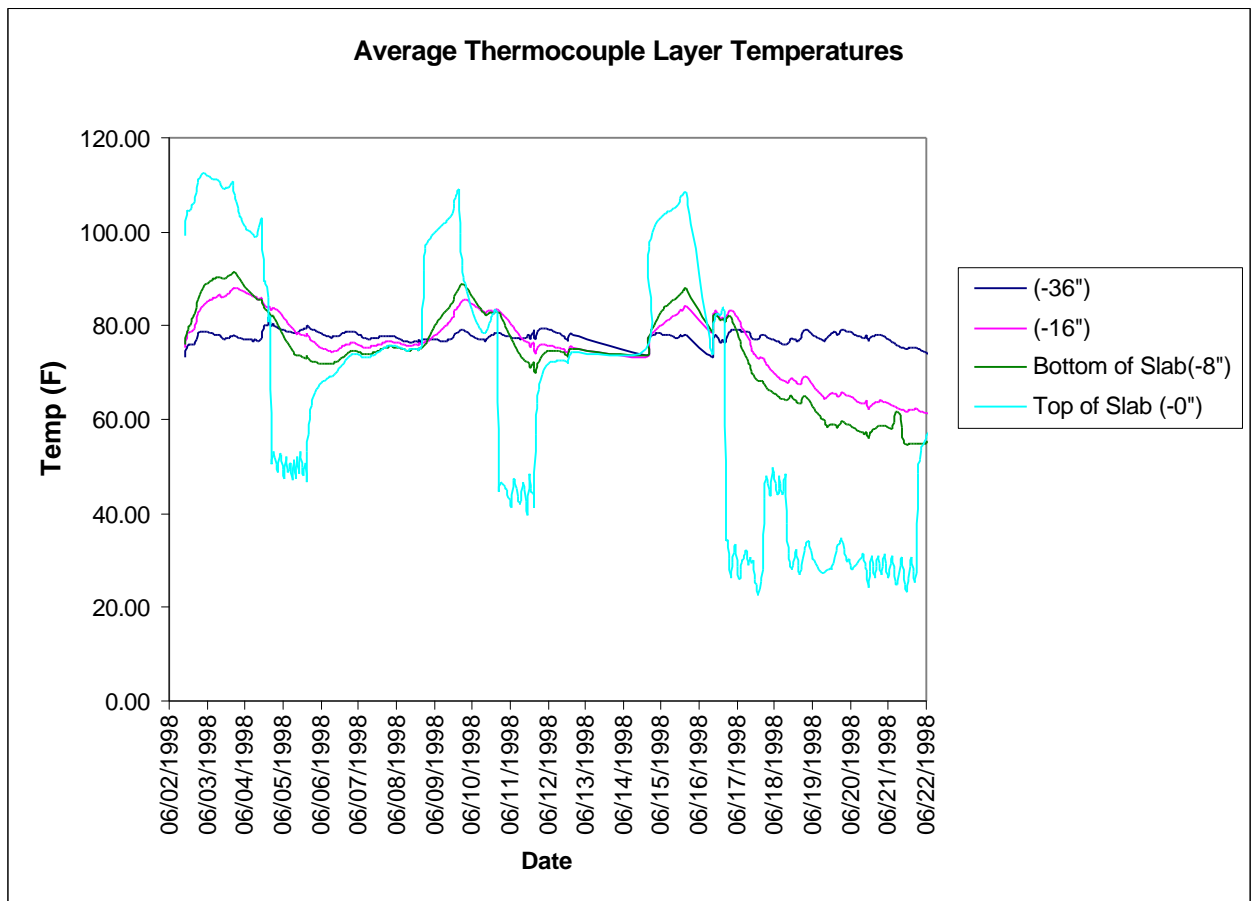


Figure 3.9 Average Thermocouple Layer Temperatures